Landmarks in Earth Reinforcement, Ochiai et al. (eds),
© 2001 Swets & Zeitlinger, ISBN 90 2651 863 3

Performance of geotextile reinforced slopes subjected to seepage flow

A. Hiro-oka, M. Kobayashi, H. Nagase & K. Shimizu
Department of civil engineering, Kyusyu Institute of Technology, Japan

H. Fujiwara
Sewage Works Bureau, Fukuoka Municipal Government (Formerly Kyushu Institute of Technology), Japan

ABSTRACT: A series of centrifuge model tests were carried out to investigate the behavior of slopes reinforced with geotextile subjected to seepage flow, and to evaluate the contribution of reinforcement to the stability of these slopes. It was found that the smaller shear deformation in the toe area of embankment and the smaller settlement and fewer crack at the top of embankment were observed with the narrower reinforcement spacing. The factor of safety obtained by means of limit equilibrium could assess the condition of a reinforced slope to a certain extent; however, it could not accurately evaluate the stability of embankments for the reason that in those stability analyses the deformation of embankment that is required to produce the reinforcement force of geotextile was not taken into account. As part of investigation in this study, the model tests were conducted with the viscous fluid in order to check the similitude in seepage phenomenon between the prototype and the model.

1 INTRODUCTION

A lot of slopes fail due to a long or heavy rain in Japan during rainy or typhoon season. Therefore, many researchers have studied on the failure mechanism of slopes due to rainfall and prediction methods of slope failure. Takemura et al. (1994) investigated the effectiveness of centrifuge model test using 1/50 scale model of embankment which object of large scale model tests conducted by Sugiyama et al. (1993), subjected to seepage flow in 50g centrifugal acceleration field. Kimura et al. (1991) carried out a series of centrifuge model tests to investigate the failure mechanism of fills subjected to various intensity of rainfall. Hiro-oka et al. (1999) studied the influence of soil shear strength and inclination of slopes on mechanism of failure due to seepage flow. Various types of grand flows in centrifuge model were studied by Goodings (1994). In many cases of these slope failures, the decrease of the slope stability was caused by the reduction of the soil strength due to the increase of its degree of saturation or the decrease of the effective stress due to the rise of ground water level in the slope. The reinforcement with geotextiles has been often adopted to increase the stability of slope. The characteristics of friction between soil and geotextile were examined by many researchers (e.g. Ingold, 1982 and Myles, 1982). Zornberg et al. (1998) conducted a series of centrifuge model tests to investigate the performance of slopes reinforced by two-types of geosynthetics and various reinforcement spacing and two-types of back fill conditions, and to evaluate the stability of slopes by means of limit equilibrium. However, the performance of geotextile reinforced slopes subjected to seepage flow has been not sufficiently understood because the mobilized reinforcement forces in addition to tensile force acted on geotextile itself were too much complicated under such condition.

In this study, a series of centrifuge model tests were carried out to investigate the behavior of slopes reinforced with geotextile subjected to seepage flow, and to check the similitude in seepage phenomenon between prototype and model in the case with the viscous fluid. In order to evaluate the stability of reinforced slopes, after making clear the friction between soil and geotextile was examined by means of direct shear test, the limit equilibrium analyses were also carried out.

2 MATERIAL PROPERTIES

2.1 *Soil material*

The artificial mixture, which consists of 50% of silty sand sampled in Kyushu Institute of Technology and 50% of Toyoura sand, and it classified as SF and the properties are shown Table 1. The internal friction angle and cohesion of soil obtained by direct shear test were also shown in Table 1.

2.2 *Geotextile*

The geotextile shown in Figure 1 was installed in the model embankment. It is non-woven fabric that consists with 100% polyester and 0.06 mm thickness.

Table 1. Physical properties and strength parameters of artificial mixture.

Specific gravity, Gs	2.67	Dry density, ρ_d (g/cm^3)		1.40
Effective grain size, D_{10} (mm)	0.13	Degree of compaction (%)		75
Uniformity coefficient, U_c	14.0	Coefficient of permeability, k ($\times 10^{-3}$ cm/s)		3.88
Sand fraction (%)	67.5			
Silt fraction (%)	25.0	Initial condition	Cohesion (kPa)	20.8
Clay fraction under 5μ (%)	7.50	w=10(%)	Angle of friction (degree)	33.0
Maximum dry density, ρ_{dmax} (g/cm^3)	1.85	Sr=100(%)	Cohesion (kPa)	4.50
Optimum moisture content, w_{opt} (%)	16.7		Angle of friction (degree)	33.0

Wide-width strip test under unconfined condition was conducted to examine the tensile strength of geotextile with 200 mm wide and 100 mm long specimen, which was based on the size of ISO 10319 tensile test. The unconfined ultimate tensile strength and the strain breakage were 0.27 kN/m and 13 % respectively. The tensile strength converted to prototype was 13.5 kN/m if it used at 50g centrifugal acceleration field.

3 DIRECT SHEAR TESTS

3.1 *Test procedures and conditions*

The direct shear tests were carried out to investigate the soil shear strength and frictional properties between soil and geotextile. Figure 2 shows the test setup with soil-geotextile shear tests. Both of shear boxes was 6 cm diameter and 1 cm depth. The porous stone, on which the filter paper and geotextile were pasted, was placed in the lower box, for the purpose of corresponding the shear surface with contact surface between soil and geotextile. The mixture with 10 % water contents, was threw into the upper shear box and compacted with dry density ρ_d=1.40 g/cm^3. The shear tests were carried out under displacement-controlled conditions that shearing at the rate of 0.25 mm/min. In the case with saturated conditions, the shear boxes were covered with vinyl bag, which filled with water, in order to keep specimen saturated during shear tests. The shear was continued until horizontal displacement reached 7 mm or shear force became constant.

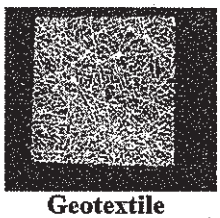

Figure 1. Geotextile.

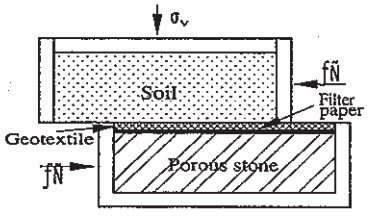

Figure 2. Direct shear tests.

3.2 *Test results and discussions*

Figure 3 shows the relationships between shear stress and effective stress obtained by direct shear tests. According to this figure, in the case with soil the internal friction angle are identical to each other condition, though the cohesion decreases as increasing the degree of saturation. On the other hands, in this figure, it is pointed out that the friction angle increases with installed the geotextile and cohesion decreases, irrespective of degree of saturation. It may be the influence of the roughness of the geotextile. It is considered that the geotextile made decrease the suction of soil at contact surface and it cause to reduce the cohesion, and increasing friction angle may be caused by the geotextile firmed the engagement with soil. However, the detail discussion could not present, because the frictional properties were depend on the combination of geotextile and soil and only one combination was investigated in this study.

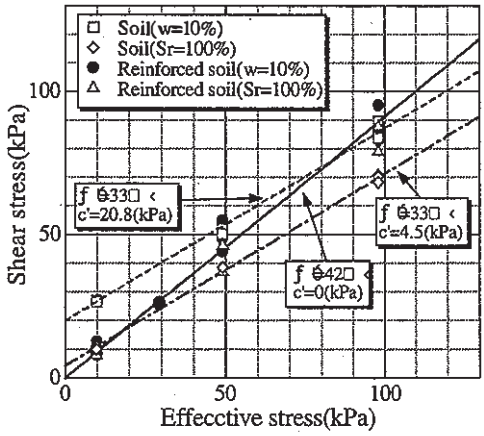

Figure 3. Relationships between shear stress and effective stress.

Table 2. Test conditions.

Test code	Type of geotextile	Tensile strength (kN/m)	Reinforcement spacing (cm)	Pore fluid
S0	-	-	-	Water
S0V	-	-	-	Viscous fluid
S3F	Non-woven fabric F	0.93 (46.5)	5.8 (290)	Water
S3FV	Non-woven fabric F	0.93 (46.5)	5.8 (290)	Viscous fluid
S6F	Non-woven fabric F	0.93 (46.5)	2.9 (145)	Water

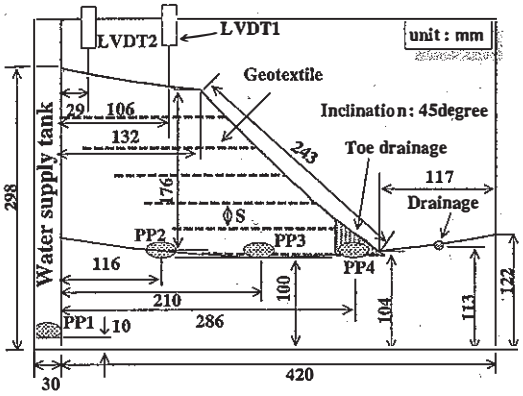

Figure 4(a). Test set up for the cases with water.

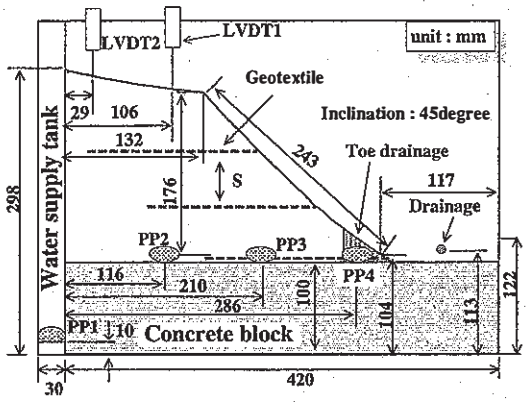

Figure 4(b). Test setup for the cases with viscous fluid.

4 CENTRIFUGE MODEL TESTS

4.1 *Test procedures and condition*

Table 2 presents the test condition in this study. Tensile strength and reinforcement spacing in the bracket in this table shows the value converted to proto type scale.

The model embankment was built in a steel-made box with 450 mm in length, 350mm in depth and 150mm in width, which has a water tank inside for supplying water to model embankment. The test setup is illustrated in Figure 4(a). To construct a base part of embankment, the mixture was placed in a model container and compacted by a bello-fram cylinder into a 2.0cm thick layer with a predetermined dry density, ρ_d=1.40 g/cm^3, and this was continue until the total thickness reached 10 cm. On the other hand, in the case with viscous fluid, a concrete block was placed in the model container as a base part shown in Figure 4(b). 3 pore water pressure transducers were placed on the top of the base part of a model embankment that corresponds to the shoulder, center and toe of a slope. After this work, the mixture was threw into the model container again and compacted by a bello-fram cylinder with 2.9cm thickness. The geotextile was installed on the 2.9 cm or 5.8cm thick layer of model ground in the case with reinforced slopes. These works were continued until the total thickness reached 30.4 cm and then the layer was cut into a model embankment with 176 mm height by using a template so that the surface of model embankment, and base ground which consist with soil in itself, have a curvature corresponding to the radial variation of the centrifugal acceleration. At the toe area, the coarse sand, which was covered with non-woven fabric, were placed as drainage. In order to reduce the friction between soil-mass and box to minimum, the inside walls and a front window was well-lubricate with silicon grease. The white Kaolin clay are painted onto the models using a template to improve observing deformation of embankments in flight. A pore water pressure transducer was placed on the bottom of water supply tank, and 2 linear variable displacement transducers (LVDTs) were placed over the top of embankment for measuring its settlement.

After completion of model embankment, the test setup was mounted on the K.I.T. Centrifuge and centrifugation was conducted at 50g. Supplying water to the water tank behind the model embankment from laboratory floor through hydraulic slip ring at a rate of 5 mm/min to carried out seepage tests and the tests were continued until slope failed clearly or the water level reached the total height of embankment. In the case with viscous fluid, although rate of supplying fluid in the water tank was identical to another series, water level in the tank has not kept increasing during seepage tests because the fluid has too much viscosity. Hence, the water level was raised 5 cm at once and left this condition alone until the output of pore pressure transducer installed model embankment was assumed to be steady.

To determine the ground water level at a lower stream, the drainage was made by holing the backside wall of model container at the height of base part of embankment.

4.2 *Test Results and Discussions*

In the cases with non-reinforcement and water, the catastrophic failure, which occurred along a large well-defined slip surface suddenly, was observed as shown in Figure 5, however, except for this case, model embankments were not failed catastrophically when the ground water level at the upper stream of embankment reached the limit height. Hence, the performances of embankment until test stopped were discussed below. Relationships between the settlements of crest of embankments (LVDT1) and piezometoric heads at the water supply tank (PP1) in the case with water were illustrated in Figure 6. The arrows in this figure indicate when the crack was observed at the top of embankments in each case. It is pointed out that both of the behaviors of the settlement until the water level in the tank reached about 10 cm are similar. It indicates that the added tensile resistance by the reinforcement requires its deforming to some extent in order to make the slope stability increase. In the case S0, higher rate of settlement with increasing head at the tank was observed than in other two cases. The stability of this slope decreased due to increasing the soil mass with rising ground water level and decreasing the shear strength with increasing the degree of saturation and these caused the lateral deformation of embankment with developing the shear deformation at toe area. Subsequently the tension crack was observed at the crest of embankment as shown in Figure 7. It is also pointed out that the smaller shear deformation in the toe area of embankment and smaller settlement and fewer cracks at the top of embankment are observed with the narrower reinforcement spacing. The reinforcement force well contributed to the stability of the slopes.

Figure 8 shows the relationships between the settlements at the top of embankment and heads at the water supply tank in the cases with viscous fluid. It is found that the settlements with raising ground water level are almost similar in S0V and S3FV. It indicates that there is no effect of reinforcement for decreasing the settlement, however, in Figure 7, which showed the observed deformation of embankment during seepage, smaller shear deformation in the toe area was observed with reinforced embankment. It implies that the tensile resistance was contributes the stability of slope. Figure 9 is comparing the profiles of the ground water surfaces recorded by photographing during seepage tests for each case. It is found that the lower ground water level at the toe area is observed in the case S3FV. It is considered that the transmitivity of non-woven fabric made increase the permeability of embankment at the stratum of installed the geotextile, especially, the lowest geotextile made the effect of toe drainage increase. Furthermore, it is pointed out that the ground water level at the toe area against the upper stream area in the cases with viscous fluid was much lower than the cases with water. It may be the influence of the viscosity of pore fluid. It is considered that the ground water surface in the model embankments determined by water level at the upper

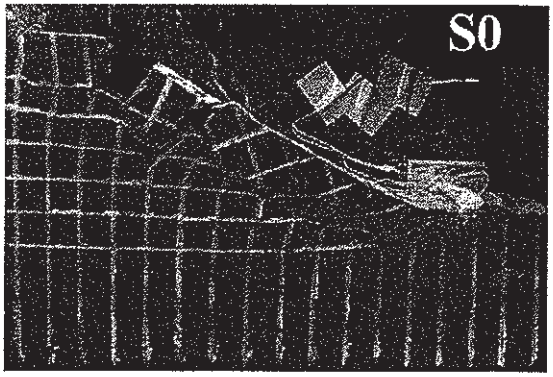

Figure 5. Final collapse of embankment (S0).

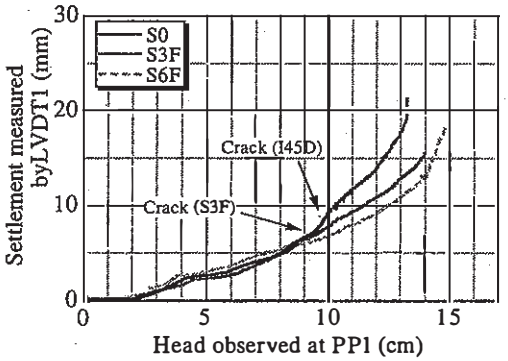

Figure 6. Relationships between the settlement at the top of embankment and head at the water supply tank.

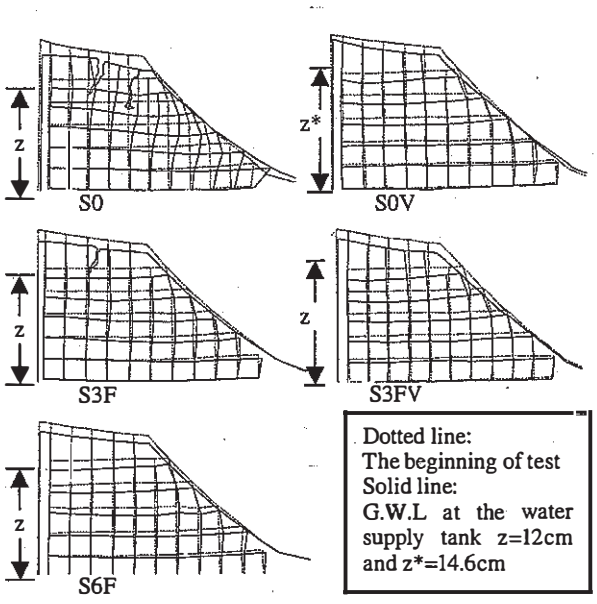

Figure 7. Observed deformation.

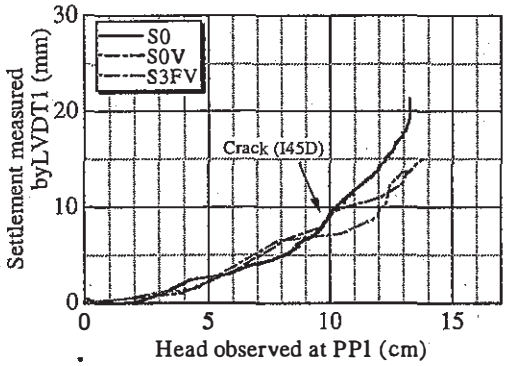

Figure 8. Relationships between the settlement at the top of embankment and head at the water supply tank.

stream if the fill consisted of well-infiltrated material or the pore fluid had less viscosity. On the other hands, the fill material had the less infiltration or pore fluid had the more viscosity, the ground water level at the lower stream might have the more effect on the profiles of ground surface in the embankment. Thus, the ground water surface in this test series was not in agreement with each other.

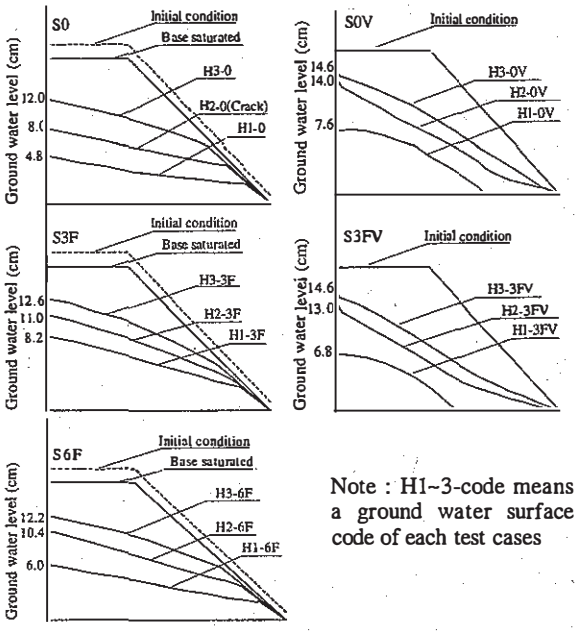

Figure 9. Variation of ground water surface of embankment.

5 STABILITY ANALYSIS

5.1 *Calculation method*

On varying conditions of ground water surface shown in Figure 9, stability analyses were attempted by means of Modified Fellenius method. In these analyses, angle of shear resistance and apparent cohesion listed in Figure 3 were adopted and calculations were made for the geometry condition just at the moment when the base layer was saturated shown in Figure 9. The ground water surface just before failure in the case S0 was adopted in S3F and S6F in order to evaluate the reinforcement force. On the other hand, in the case with viscous fluid, the ground water surfaces just before the end of test were adopted in the calculations.

According to Figure 10, the factor of safety was calculated by following formula,

$$F_S = (\Sigma M_R + \Sigma \Delta M_R) / \Sigma M_D \qquad (1)$$

here, M_R and M_D, M_R means the moments of resisting slope failure and the moments of driving slope failure, and the moments of resisting slope failure by reinforcement respectively. The evaluations of reinforcements are explained in detail below. On the assumption that the frictional resistance acted on both of surface of geotextile, to determine the direction of pull-out, the sums of frictional resistance R_{1j} corresponding to the effective overburden-pressure inside the slipping soil-mass and R_{2j} corresponding to the one outside it were calculated. In order to decide whether geotextile pull out or break at failure, the minimum value of frictional resistance and tensile strength of geotextile T_f are compared. The minimum value of those was added to the moment of resisting slope failure by reinforcement M_R as followed formula,

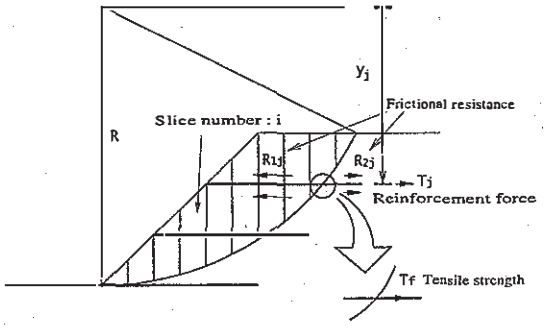

Figure 10. Evaluation of reinforcement.

$$F_S = \frac{\Sigma(c'l + W_i' \cos\alpha_i)R + \Sigma Min\left[T_f, R_{1j}, R_{2j}\right] y_j}{\Sigma W_i \sin\alpha_i \cdot R} \qquad (2)$$

here, i means a number of slice and W means a weight of slice.

The cracks observed at the top of embankment in the case S0 and S3 were taken into account in the analysis, which on the assumption that the one crack reach the uppermost geotextile in the case S3 each other.

5.2 *Results and discussion*

The minimum safety factors and critical circles in several cases were illustrated in Figure 11 and 12. It is pointed out that the critical circles in the case S0 and S3F are similar each other. It implies that the stability of embankment in S3F decreased to a certain extent though the catastrophic failure was not observed in this case. In the case S6F, it is found that the critical circle is largest and crosses the uppermost geotextile near its edge. It suggests that the internal stability of this embankment is sufficient.

In the cases with viscous fluid, it is found that these embankments were still stable according to the values minimum safety factor. On the critical circle of S3FV, its excluding from the reinforcement area of embankment indicates the stability of embankment was enough like a case S6F. It may be caused by the profiles of ground water surface in the embankments, especially, the ground water level at the toe are of the slopes. It implies that to keep the water level at the toe area low make the stability of embankment subjected to seepage flow increase.

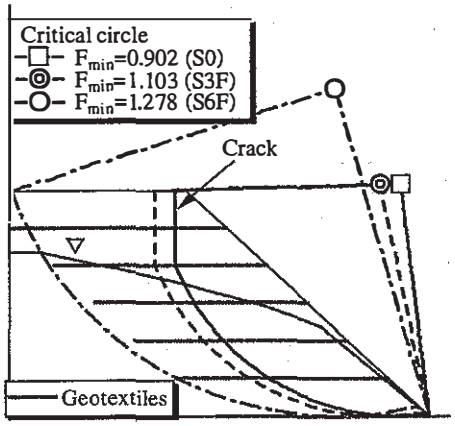

Figure 11. Critical circles and minimum safety factors in water series.

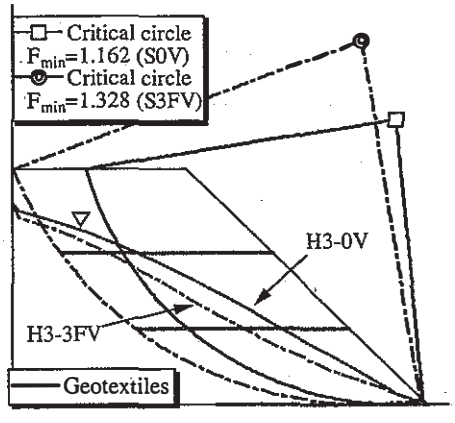

Figure 12. Critical circles and minimum safety factors in viscous fluid series.

6 CONCLUSIONS

A series of centrifuge model tests were conducted to investigate the performance of geotextile reinforced slopes subjected to seepage flow and to try the evaluation of stability of reinforced embankment by means of limit equilibrium. Following conclusions were obtained.

A smaller shear deformation in the toe area of embankment and smaller settlement and fewer cracks at the crest of embankment were observed with the narrower reinforcement spacing of reinforced slopes subjected to seepage flow. However, the added tensile resistance by the reinforcement requires its deforming to some extent in order to make the slope stability increase.

The factors of safety obtained by means of limit equilibrium could assess the condition of a reinforced slope to a certain extent. However, it could not accurately evaluate the stability of embankments for the reason that in those stability analysis the deformation of embankment that is required to produce the reinforcement force was not taken into account.

REFERENCES

Goodings, D.J. 1994. Implication of changes in seepage flow regimes for centrifuge models. Proc. ofCentrifuge'94: 393-398, Rotterdam: Balkema.

Hiro-oka, A., M.Kobayashi, H.Nagase & K.Shimizu 1999. Centrifugal modeling of slope failure due to seepage flow. Proc. Symp. Recent Development of Theory and Practice in Geotechnology: 150-157.

Ingold, T.S. 1982. Some observation on the laboratory measurement of soil-geotextile bond. Geotechnical Testing Journal, Vol.5, No.3/4: 57-67.

Kimura, T., J.Takemura, N.Suemasa & A.Hiro-oka 1991. Failure of fill due to rain fall. Proc, of Centrifuge'91: 509-516, Rotterdam: Balkema.

Myles, B. 1982. Assessment of soil fabric friction by means of shear. Second International Conference on Geotextiles, Las Vegas: 787-791.

Sugiyama, T., H.Muranishi, K.Kagawa, K.Kusano & K. Mizushima 1993. Estimating the timings collapse of embankment slope based on experiment of large scale model. Proc. Annual Meeting JSSMFE, 2: 2167-2168.

Takemura, J., T.Kimura, A.Hiro-oka & H.Muranishi 1994. Failure of embankments due to seepage flows and its countermeasure. Proc. of Centrifuge'94: 575-580, Rotterdam: Balkema.

Zornberg, J.G., N.Sitar, J.K.Mitchell 1998. Performance of geosynthetic reinforced slopes at failure. Journal of Geotechnical and Geoenvironmental engineering, Journal of Geotechnical Engineering and Geoenvironmental Engineering, Vol.124, No.8: 670-683.

Zornberg, J.G., N.Sitar, J.K.Mitchell 1998. Limit equilibrium as basis for design of geosynthetic reinforced slopes. Journal of Geotechnical and Geoenvironmental engineering, Journal of Geotechnical Engineering and Geoenvironmental Engineering, Vol.124, No.8: 684-698.